

LETTER

Analysis of tungsten migration from the C-MOD divertor; prediction of high redeposition rate, and code validation progress

J.N. Brooks

Center for Materials under Extreme Environment, School of Nuclear Engineering, Purdue University, West Lafayette, IN, USA

Received 9 November 2012, accepted for publication 14 February 2013

Published 1 March 2013

Online at stacks.iop.org/NF/53/042001**Abstract**

For acceptable magnetic fusion reactor performance it is critical that net erosion of high- Z plasma facing material be much less than gross erosion. A detailed simulation of outer divertor-sputtered tungsten migration in the C-MOD tokamak, over an extended plasma campaign, shows a high ratio, $\sim \times 10$, of gross/net erosion, no core plasma contamination, and moderate transport of tungsten to lower divertor regions. These code predictions agree well with the available data. This is encouraging for high- Z material use in ITER and future fusion devices.

1. Experiment

As reported in [1, 2] tungsten tiles in the centre of the Alcator C-MOD outer divertor were exposed to several thousand plasma discharges at widely varying plasma conditions. The tungsten tiles replaced the normal molybdenum tiles and were symmetric toroidally and 3 cm wide poloidally (see figure 1 of [1]). Post-exposure W deposition on the Mo portions of the divertor was measured by an external MeV ion beam (PIXE, PIGE). While gross erosion was not measured directly (e.g. by spectroscopy), integration of the post-exposure W deposition showed that a net effective thickness $4 \times 10^{21} \text{ W m}^{-2} \approx 60 \text{ nm}$ was removed from the tungsten tiles. Top-to-bottom tungsten migration was observed on the near-vertical outer divertor, and some deposition observed on the inner divertor.

2. Modelling

The modelling goal is to compute the tungsten tile sputter erosion and impurity transport with key focus on the gross/net erosion ratio, net erosion being the difference between sputtering and redeposition. The methodology is similar to that of a recent analysis for a C-MOD all-molybdenum divertor campaign [3]. In particular, a REDEP/WBC code package (3D, full kinetic, Monte Carlo) sputtering erosion/redeposition simulation, using sheath and sputter code calculations, is

performed for the C-MOD tungsten test section divertor campaign.

The modelled plasma is a deuterium plasma with data-inferred 1% B^{3+} particle flux to the divertor, with strike point (peak particle flux) on the W tile. The plasma shots have been characterized into eight canonical types totalling 2284 s, with strike point electron temperature ranging from $T_e \sim 5\text{--}45 \text{ eV}$, electron density $\sim 3 \times 10^{19}\text{--}1 \times 10^{20} \text{ m}^{-3}$ [1, 2], and fairly constant resulting D^+ flux of $\sim (2\text{--}3) \times 10^{22} \text{ m}^{-2} \text{ s}^{-1}$. Other (numerous) discharges with $T_e < 5 \text{ eV}$ do not contribute to sputter erosion, per this analysis. Plasma shot probe etc data input to WBC includes exposure times, and per canonical shot T_e , Ne, and B -field poloidal spatial variation in the outer divertor region.

Coupled WBC and BPHI-3D (3D, kinetic-plasma, Poisson-solver, sheath code) calculations determine the dual-structure (magnetic + Debye) tokamak-type sheath conditions and ion impingement velocities at the tungsten tiles. ITMC-DYN binary collision approximation (BCA) sputter code [4, 5] computations [6] give the energy-dependent W sputter yields for D, B, and W impingement, and the sputtered atom energy/angular distribution functions. Pure tungsten is assumed. The normalized sheath potential, sheath structure, and average ion elevation incidence angle— 65° from normal for boron, 25° for tungsten—are found to be reasonably constant over the shot types.

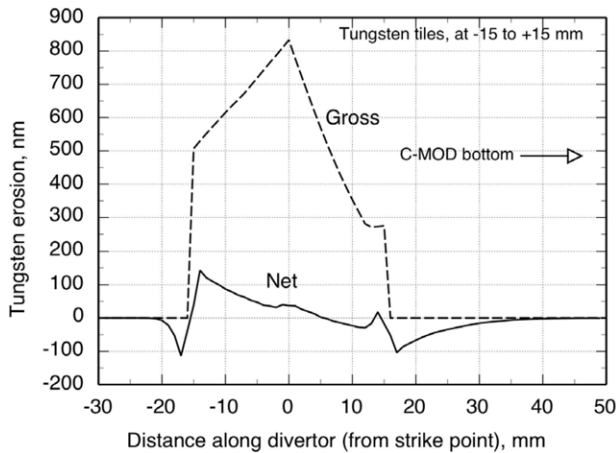


Figure 1. Campaign-integrated gross and net tungsten erosion along C-MOD tokamak outer divertor, for reference case plasma conditions.

Computed B^{3+} impingement energies vary from about 100–700 eV over the campaign (for $T_e > 5$ eV), such energies arising from pre-sheath B thermalization with the majority D plasma, and sheath acceleration. B–W sputter yields (using KrC potential in ITMC [4,5]) vary from ~ 0.01 to 0.30 for this energy range, being e.g., 0.07 at 250 eV [6]. Incident D^+ energies are below threshold for W sputtering, per ITMC results (and literature data). (Charge exchange D^0 flux estimates are not available but significant sputtering from this source is not expected for the C-MOD plasma conditions, due to high threshold energies for D on W sputtering).

The reference case plasma has no pre-sheath radial electric field. An alternative case examined is with a fixed radial field ($\sim \perp$ to outer divertor) of 3000 V m^{-1} , presumed due to the cross-field electron temperature gradient [7].

REDEP/WBC computes the full-kinetic, 3D, sputtering, ionization and transport of surface material atoms/ions due to Lorentz force motion and velocity-changing and charge-changing collisions with the background plasma, e.g., as described in [8]. The present simulation uses $\sim 10^6$ particle histories per case (including self-sputtering); tungsten particles terminate upon divertor redeposition or being lost from the divertor region to the core plasma (none for this analysis).

While not a critical issue for the present purposes we note that *mixed-material* effects were not simulated here (due to funding limitations). This would be needed for a more complete analysis of the W/Mo divertor—in terms of W surface evolution/response due to Mo deposition, and re-sputtering of deposited W on the Mo tiles.

3. Simulation results

Results are shown in figures 1, 2 and table 1. Figure 1 shows the campaign-integrated gross and net tungsten erosion along the outer divertor. We see a peak gross erosion of ~ 800 nm, and W tile-averaged rate of ~ 600 nm. The average net erosion is about 40 nm, in good agreement with the data—particularly considering various uncertainties in the plasma parameters—and an order of magnitude less than the gross rate. Most erosion is due to boron impingement, with self-sputtering being about

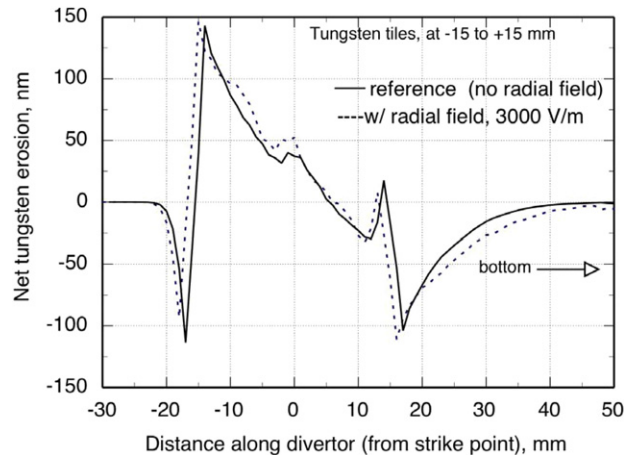


Figure 2. Campaign-integrated net tungsten erosion along C-MOD outer divertor. Reference case (no radial electric field) and with radial electric field. No major difference observed.

a 30% effect (from redeposited W ions in the ~ 2.5 average charge state with ~ 300 eV average energy). The simulation shows top-to-bottom migration of W along the divertor, almost no transport of W above the W tiles (other than to a ~ 5 mm transition zone), and no core plasma W contamination, all in good agreement with the data.

The non-contamination is due to 100% local redeposition to the divertor; due to a combination of near-surface sputtered W atom ionization (~ 0.5 mm campaign-integrated mean free path), high W-ion collisionality with the incoming plasma, and electric field acceleration and gyro-rotation back to the surface.

Figure 2 shows the net erosion profile in finer detail, both for the reference case and the non-zero radial electric field case. From this figure and table 1, there is seen to be some but not major effect of a radial field. This is due to the short (several μs) average W-ion transit time from ionization to redeposition, compared to the much longer time needed for significant poloidal motion due to the radial electric field, mostly via $E \times B$ drift.

As mentioned, mixed-material effects are not treated here. However, by extrapolation from a recent C/Mo mixed-material DIII-D analysis [9] such effects would tend to smooth out the high variations shown for the W/Mo transition regions, i.e. at/near ± 15 mm, because of re-sputtering of at least some of the W deposited on the Mo. But this would not change the fundamental picture. Likewise, a sensitivity analysis showed no major changes for several model parameters including ± 1 boron ion charge state difference, ± 1 cm strike point location, and factor of 2 difference in W ionization rate coefficients.

4. Discussion

Migration of sputtered tungsten to the inner divertor is not predicted by these simulations, with or without a radial electric field. However, such migration may conceivably have been caused by re-sputtering of tungsten deposited on lower portions of the outer divertor; resulting transport times being longer than near the divertor centre, due to a less collisional plasma. Outer-to-inner divertor tungsten transport was also seen in JT-60 [10], possibly from similar causes. Future work can examine this for C-MOD.

Table 1. C-MOD tungsten campaign simulation; REDEP/WBC code package results compared to some available data.

Parameter	Simulation Reference case	Simulation $E_{\text{radial}} = 3000 \text{ V m}^{-1}$	Data [1, 2]
Gross erosion, W tiles (nm)	588 (tile-average)	533	—
Net tungsten erosion (nm)	42 (tile-average)	50	~60 nm
Tungsten deposition, 3 cm below strike point (m^{-2})	10.4×10^{20}	16.5×10^{20}	$\sim 10 \times 10^{20}$

5. Conclusions

This analysis and code/data comparison for the C-MOD tungsten divertor campaign shows generally encouraging results:

- Factor of $\sim \times 10$ difference between predicted gross and net tungsten erosion.
- Good code/data net erosion comparison. (In contrast to a Mo campaign analysis [3], for reasons not clear but possibly due to improved diagnostics.)
- Predicted transport of tungsten along the divertor in line with data and tending to confirm the physical picture of redeposition due to near-surface ionization and transport from Lorentz forces and impurity-plasma collisions, and resulting selective migration towards the private flux region along downward-pointing poloidal magnetic field lines.

The C-MOD campaign results are thus viewed as positive for ITER tungsten divertor performance, where high redeposition is predicted and required [11], and likewise for DEMO and Commercial fusion tokamaks.

Future work will hopefully be enabled on this subject with mixed-material analysis and focus on transport mechanisms from the outer-to-inner divertor.

Acknowledgments

This work was supported by the US Department of Energy, Office of Fusion Energy.

References

- [1] Barnard H.S., Lipschultz B. and Whyte D.G. 2011 *J. Nucl. Mater.* **415** S301
- [2] Barnard H.S. 2009 External proton beam analysis of plasma facing materials for magnetic confinement fusion applications *Masters Thesis* Massachusetts Institute of Technology
- [3] Brooks J.N., Allain J.P., Whyte D.G., Ochoukov R. and Lipschultz B. 2011 *J. Nucl. Mater.* **415** S112
- [4] Hassanein A. 1985 *Fusion Technol.* **8** 1735
- [5] Sizyuk T. and Hassanein A. 2010 *J. Nucl. Mater.* **404** 60
- [6] Hassanein A. and Sizyuk T. 2012 personal communication
- [7] Whyte D.G. 2012 personal communication
- [8] Brooks J.N. 2002 *Fusion Eng. Des.* **60** 515
- [9] Brooks J.N., Hassanein A. and Sizyuk T. 2012 Advanced simulation of mixed-material erosion/evolution and application to low and high-Z containing plasma facing components *PSI-20 Conf. (Aachen, Germany, 2012)*; *J. Nucl. Mater.* at press [10.1016/j.jnucmat.2013.01.142](https://doi.org/10.1016/j.jnucmat.2013.01.142)
- [10] Ueda Y. *et al* 2009 *Nucl. Fusion* **49** 065027
- [11] Brooks J.N. *et al* 2009 *Nucl. Fusion* **49** 035007